

Electron transport in AlGaN–GaN heterostructures grown on 6H–SiC substrates

R. Gaska, J. W. Yang, A. Osinsky, Q. Chen, and M. Asif Khan^{a)}
APA Optics, Inc., Blaine, Minnesota 55449

A. O. Orlov and G. L. Snider
Department of Electrical Engineering, University of Notre Dame, Notre Dame, Indiana 46556

M. S. Shur
Department of Electrical, Computer, and Systems Engineering, Rensselaer Polytechnic Institute, Troy, New York 12180-3590

(Received 26 August 1997; accepted for publication 10 December 1997)

We investigated two-dimensional electron transport in doped AlGaN–GaN heterostructures (with the electron sheet concentration $n_s \approx 10^{13} \text{ cm}^{-2}$) grown on conducting 6H–SiC substrates in the temperature range $T=0.3\text{--}300$ K. The electron mobility in AlGaN–GaN heterostructures grown on SiC was higher than in those on sapphire substrates, especially at cryogenic temperatures. The highest measured Hall mobility at room temperature was $\mu_H = 2019 \text{ cm}^2/\text{V s}$. At low temperatures, the electron mobility increased approximately five times and saturated below 10 K at $\mu_H = 10250 \text{ cm}^2/\text{V s}$. The experimental results are compared with the electron mobility calculations accounting for various electron scattering mechanisms. © 1998 American Institute of Physics. [S0003-6951(98)04106-0]

Monte Carlo simulations predict a high peak velocity, v_p , high saturation velocity, v_s , and a relatively high electron mobility, μ , in GaN doped at 10^{17} cm^{-3} (see Refs. 1–5). More recently, transient Monte Carlo calculations⁶ showed that this material should exhibit ballistic and overshoot transport, which is expected to be even more pronounced than in GaAs, but at much higher voltages. Experimental data and mobility calculations for the two-dimensional (2D) electron gas at the AlGaN/GaN heterointerface show that the 2D electron mobility is much higher than that for bulk GaN^{7–9} and decreases relatively little with doping compared to AlGaAs/GaAs structures. A higher value of the mobility in the 2D gas is primarily related to the decrease of the ionized impurity scattering caused by the separation from the ionized donors and by screening effects in a high density 2D electron gas.⁶

It was demonstrated recently^{9,10} that 2D electron mobility in AlGaN–GaN heterostructures can be significantly enhanced by growing epilayer structures on 6H–SiC substrates. The enhancement was primarily attributed to a smaller lattice mismatch between SiC and GaN, and resulted in a better quality of AlGaN–GaN interface. The highest reported Hall mobilities in the heterostructures on silicon carbide at $T=77$ K are 5413 (Ref. 9) and 5600 $\text{cm}^2/\text{V s}$,¹⁰ whereas in similar structures grown on sapphire substrates the mobility was close to 4000 $\text{cm}^2/\text{V s}$.⁸

In this letter, we present our most recent experimental data which demonstrate that the electron mobility in the 2D electron gas at the AlGaN–GaN heterointerface may be substantially higher than was believed before. We report low temperature mobility values of over 10 000 $\text{cm}^2/\text{V s}$.

The epilayer structure was grown by the low pressure metalorganic vapor pressure epitaxy¹¹ on n -type 6H–SiC

substrates. A 150 nm AlN layer growth on silicon carbide was followed by the deposition of a 0.5 μm nominally undoped GaN layer, 50 nm n -GaN layer with an estimated doping level $n = 5 \times 10^{17} \text{ cm}^{-3}$. Finally, the GaN layer was capped with a 50 nm $\text{Al}_{1.20}\text{Ga}_{0.80}\text{N}$ barrier layer. The piezoeffect^{12,13} and the barrier and channel doping resulted in a large electron sheet concentration $n_s = 1.3 \times 10^{13} \text{ cm}^{-2}$ determined from Hall measurements using the van der Pauw contact configuration. Low temperature Hall measurements were performed on the Hall bar with geometry factor $\gamma = 7$ (ratio of the bar length to the bar width) obtained by reactive ion etching of the mesa. The contact formation was the same as that reported in Ref. 10. The low temperature transport measurements were performed using the standard ac lock-in technique in the constant current mode. The current through the device was 100 nA at 22 Hz. The sample was mounted in the vacuum chamber, which allowed us to perform measurements in the wide range of temperatures and magnetic fields.

We performed the Hall measurements in the temperature range from 300 mK to 300 K. The low temperature experiments were carried out in the magnetic fields up to 9 T. We determined that the electron sheet concentration drops by approximately 25% with a decrease in the sample temperature from 300 to 100 K and remains unchanged at lower temperatures. The Hall measurements using van der Pauw contact configuration yielded the electron sheet concentrations and mobilities $n_s = 1.3 \times 10^{13} \text{ cm}^{-2}$, $\mu = 2019 \text{ cm}^2/\text{V s}$, and $n_s = 10^{13} \text{ cm}^{-2}$, $\mu = 8583 \text{ cm}^2/\text{V s}$ at $T=300$ K, and $T=77$ K, respectively. These values are in good agreement with the results we obtained from the independent measurements on the Hall bar. Figure 1(a) shows resistances R_{xx} and R_{xy} measured at liquid helium temperature $T=4.2$ K. We extracted the electron sheet concentration from simultaneous measurements of the Shubnikov–de Hass oscillations, $n_{s,H}$, [Fig. 1(b)] and of the $R_{xy}(H)$ with slope determined by $n_{s,H}$ [see Fig. 1(a)]. The electron concentration

^{a)}Current address: Dept. of Electrical and Computer Engineering, University of South Carolina, Columbia, SC 29208.

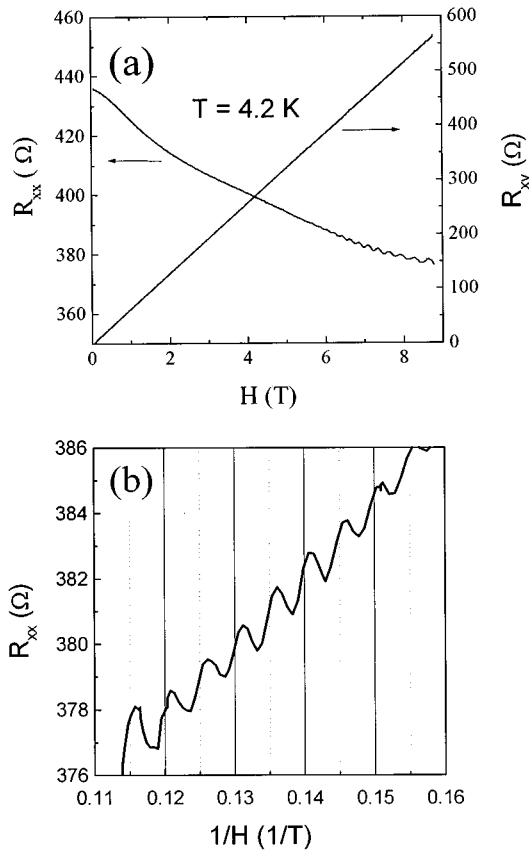


FIG. 1. (a) Hall constants R_{xx} and R_{xy} vs magnetic field at liquid helium temperature $T=4.2$ K; (b) shows Shubnikov–de Haas oscillations in quantizing magnetic fields.

in 2D gas extracted from these measurements is

$$n_{sH} = \frac{H}{R_{xy}e} \approx n_{sS-H} = \frac{2e}{h\Delta\left(\frac{1}{B}\right)} \approx 0.97 \times 10^{13} \text{ cm}^{-2},$$

where H and B are magnetic field intensity and magnetic flux density, e is electron charge, and h is the Planck constant. The electron sheet concentration remains unchanged up to the magnetic fields of 9 T [Fig. 2(a)]. The measured $\mu(H)$ dependence at $T=4.2$ K yields the Hall mobility close to $\mu_H=10\,500 \text{ cm}^2/\text{V s}$ at 1.0 T [Fig. 2(b)]. The electron Hall mobility at $H=1$ T and $T=77$ K was approximately $8600 \text{ cm}^2/\text{V s}$, which is very close to the $8583 \text{ cm}^2/\text{V s}$ obtained from the van der Pauw–Hall measurements. A further increase in the Hall mobility with a temperature decrease was observed until approximately 10 K [see Fig. 2(b)]. At lower temperatures, the Hall mobility becomes temperature independent with the value $\mu_H=10250 \pm 100 \text{ cm}^2/\text{V s}$.

Even though our results yield reasonable values for μ_H and n_s , we would like to emphasize unusual measured dependencies $R_{xx}(H)$. As one can see from Fig. 1(a), we observe a large negative magnetoresistance in high magnetic fields. In similar AlGaIn/GaN structures, Knap *et al.*⁸ observed a large positive magnetoresistance in magnetic fields up to 4 T followed by a less pronounced negative magnetoresistance in higher magnetic fields. They did not give any explanation of this effect, which remains unclear.

Figure 3 compares the measured values of the Hall mo-

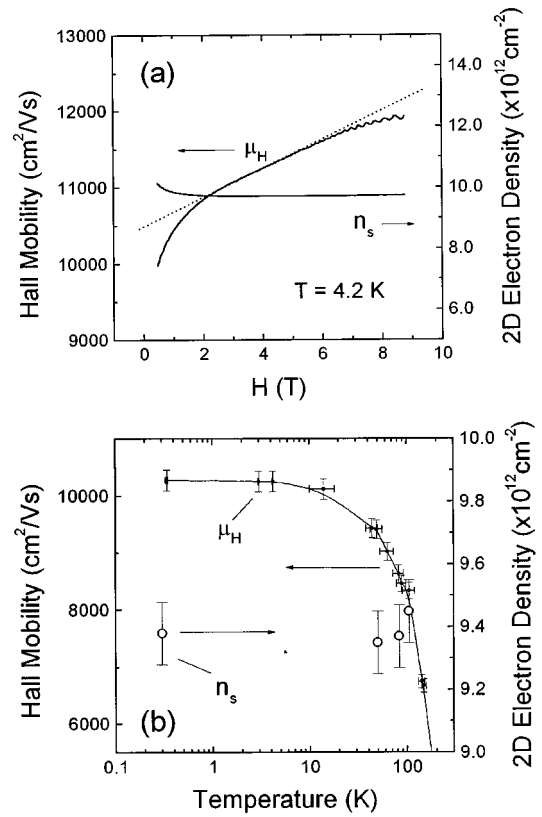


FIG. 2. (a) Electron Hall mobility, μ_H , and sheet concentration, n_s , vs magnetic field intensity at temperature $T=4.2$ K; (b) Electron Hall mobility and sheet concentration as a function of temperature measured at magnetic field intensity $H=1$ T.

bility with the results of the calculations, which use the formulas derived in Ref. 6. The theory developed in Ref. 6 exploited conventional three-dimensional (3D) electron scattering rates for all scattering mechanisms. However, the 2D effects have been accounted for by using a much higher electron concentration in the channel than the ionized impurity concentration. This accounts for a spatial separation of electrons from ionized impurities in the wide-band-gap barrier

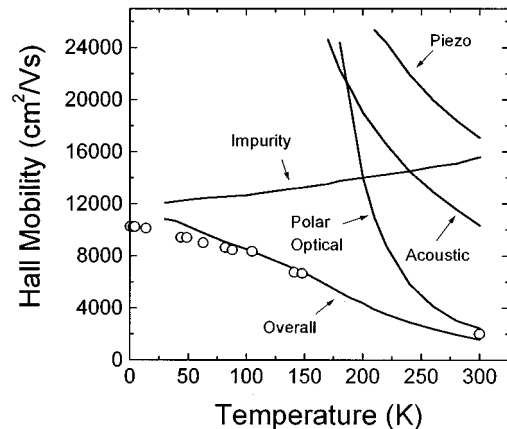


FIG. 3. Measured (open circles) and calculated (solid lines) Hall mobility as a function of sample temperature. The results of calculations account for electron scattering by optical and acoustic phonons, piezoelectric and impurity scattering.

layer and for the screening of the ionized impurity scattering in the channel—the two most important effects distinguishing the mobility of the 2D electron gas from the 3D mobility. Such an approach gave a reasonable agreement with the calculations done for GaAs and was expected to be valid for the polar optical scattering in GaN.¹ Parameters used in the calculation are: acoustic deformation potential, $\epsilon_{ac}=8.3$ eV; relative static dielectric constant, $\epsilon_0=8.9$; high frequency dielectric constant, $\epsilon_s=5.5$, effective electron mass, $m_n=0.22 m_0$, energy gap $E_g=3.4$ eV, optical phonon energy, $E_o=0.0912$ eV, elastic modulus, $c_L=2.65 \times 10^{11}$ N/m²; $c_T=4.42 \times 10^{10}$ N/m²; piezoelectric constant, $\epsilon_{14}=0.375$ C/m². Also, we assumed that the Hall factor for the piezoelectric scattering is 1.12.¹⁴

As can be seen from Fig. 3, the effective electron concentration and ionized impurity concentration primarily affect the low temperature mobility values. Our calculations qualitatively agree with experimental data. They show that the room temperature mobility values are primarily determined by the polar optical scattering and acoustic scattering. The mobility in the intermediate temperature range is strongly affected by the acoustic scattering. The quantitative agreement at room temperature cannot be reached by manipulating the values of ionized impurities and/or effective electron concentration. The possible reasons may include screening of polar optical scattering, a possible effect of localized phonons on the polar optical scattering rate, and an inaccuracy related to using 3D scattering rates. The measured room temperature mobility reaches 2019 cm²/V s, which is much larger than for comparably doped silicon (approximately 500 cm²/V s)² and about half of that for a comparably doped GaAs (approximately 4000 cm²/V s).⁹ Because of the very high electron concentration at the heterointerface, such (or even a higher) value of the mobility can be achieved even in a doped channel with a fairly large donor concentration, N_d , in GaN (the values of $N_d=2.5 \times 10^{17}$ cm⁻³ and volume electron concentration, $n=7 \times 10^{18}$ cm⁻³ were used in the calculation). Since the peak and saturation velocities in GaN are much higher than those in GaAs, these results mean that deep submicron GaN-based devices can outperform GaAs-based transistors. This prediction is consistent with our recent experimental results, which show very high drain current and transconductance values (over 1 A/mm and 180 mS/mm, respectively) for doped channel GaN-based high electron mobility transistors (HEMTs).¹⁵

The observed increase in the Hall mobility in the AlGaIn/GaN high field effect transistors (HFETs) grown on SiC substrates (compared to the HFETs grown on sapphire substrates) is especially pronounced at cryogenic temperatures. This can be explained by a better material quality of GaN grown on SiC substrates because of much smaller lattice mismatch between AlGaIn and SiC. A better material quality may manifest itself in a smaller dislocation density and/or in a less pronounced columnar structure. The dislocation density in GaN grown on sapphire is quite high (in the range 10^8 – 10^{10} cm⁻²).¹⁶ This material also has a pronounced columnar structure (called ordered polycrystalline microstructure¹⁶). The recent piezoresistivity studies on AlGaIn/GaN heterostructures revealed the existence of the

domain structure formed at the heterointerface caused by the face changes between gallium and nitrogen atomic planes at the heterointerface.¹⁷ All these effects may affect the 2D electron mobility, especially at cryogenic temperatures. The mobility limited by the dislocations is roughly proportional to temperature.¹⁸ The polycrystalline structure leads to the observation of the “mobility edge”¹⁹ and may result in the exponential temperature dependence of the mobility with a very small, concentration-dependent activation energy.²⁰ The scattering mechanisms related to the material imperfections should be much more pronounced at cryogenic temperatures. Hence, our data show a better material quality of GaN grown on SiC substrates.

In conclusion, we report on the record values of the Hall mobility in GaN-based heterostructures. A significantly higher mobility was achieved in the structures grown on 6H–SiC substrates compared to those grown on sapphire, especially at low temperatures. The qualitative analysis of our data shows that polar optical and acoustic scattering are two dominant electron scattering mechanisms at room temperature at high sheet electron carrier concentrations.

This work has been supported by the Office of Naval Research under Contract No. N00014-97-C-0033 (Project Monitor Dr. Colin Wood), and partially supported by BMDO (Program Manager Dr. Kepi Wu). The authors are grateful to Professor M. Dyakonov for illuminating discussions.

¹M. A. Littlejohn, J. R. Hauser, and T. H. Glisson, *Appl. Phys. Lett.* **26**, 625 (1976).

²B. Gelmont, K. S. Kim, and M. Shur, *J. Appl. Phys.* **74**, 1818 (1993).

³M. Shur, B. Gelmont, C. Saavedra-Munoz, and G. Kelner, in *Proceedings of the 5th Conference on Silicon Carbide and Related Compounds* (Institute of Physics Publishing, Bristol, 1994), Ser. No. 137, p. 465.

⁴R. P. Joshi and P. K. Raha, in *Proceedings of the 5th Conference on Silicon Carbide and Related Compounds* (Institute of Physics Publishing, Bristol, 1994), Ser. No. 137, p. 687.

⁵M. S. Shur, B. Gelmont, and M. Asif Khan, *J. Electron. Mater.* **25**, 777 (1996).

⁶U. V. Bhapkar and M. S. Shur, *J. Appl. Phys.* **82**, 1655 (1997).

⁷M. S. Shur, B. Gelmont, and M. Asif Khan, *J. Electron. Mater.* **25**, 777 (1995).

⁸W. Knap, S. Contreras, H. Alause, C. Skierbiszewski, J. Camassel, M. Dyakonov, J. Yang, Q. Chen, M. Asif Khan, M. L. Sadowski, S. Huant, F. H. Yang, M. Goiran, J. Leotin, and M. S. Shur, *Appl. Phys. Lett.* **70**, 2123 (1996).

⁹C. F. Lin, H. C. Cheng, J. A. Huang, M. S. Feng, J. D. Guo, and G. C. Chi, *Appl. Phys. Lett.* **70**, 2583 (1997).

¹⁰R. Gaska, Q. Chen, J. Yang, A. Osinsky, M. Asif Khan, and M. S. Shur, *IEEE Electron Device Lett.* **18**, 492 (1997).

¹¹Q. Chen, R. Gaska, M. Asif Khan, M. S. Shur, A. Ping, I. Adesida, J. Burm, W. J. Schaff, and L. F. Eastman, *Electron. Lett.* **33**, 637 (1997).

¹²P. M. Asbeck, G. J. Sullivan, E. T. Yu, S. S. Lau, and B. McDermott, *DRC'97*, Fort-Collins, CO, 1997, p. VB5.

¹³R. Gaska, J. Yang, A. Osinsky, A. Bykhovski, and M. S. Shur, *Appl. Phys. Lett.* **72**, 64 (1998).

¹⁴B. Gelmont and M. S. Shur, *J. Appl. Phys.* **78**, 2846 (1995).

¹⁵R. Gaska, J. Yang, A. Osinsky, M. Asif Khan, and M. S. Shur (unpublished).

¹⁶S. D. Hersee, J. C. Ramer, and K. J. Malloy, *MRS Bull.* **22**, 45 (1996).

¹⁷R. Gaska, J. W. Yang, A. Osinsky, A. Bykhovski, M. S. Shur, V. V. Kaminski, and S. Soloviov, *Appl. Phys. Lett.* **71**, 3817 (1997).

¹⁸B. P. Pödör, *Phys. Status Solidi* **16**, K167 (1966).

¹⁹B. Heying, X. H. Wu, S. Keller, Y. Li, D. Kapolnek, B. P. Keller, S. P. Denbaars, and J. S. Speck, *Appl. Phys. Lett.* **68**, 643 (1996).

²⁰C. H. Seager, *Annu. Rev. Mater. Sci.* **15**, 271 (1985).